AD-A107 544 WISCONSIN UNIV-MADISON DEPT OF CHEMISTRY F/G 9/1
EFFECTS OF TEMPERATURE ON EXCITED-STATE DESCRIPTIONS OF LUMINES--ETC(U)
OCT 81 A B ELLIS, B R KARAS N000014-78-C-0633
UNCLASSIFIED TR-7 NL

END
DATE FILMED
12 81
DTIC

OFFICE OF NAVAL RESEARCH

Contract No. N00014-78-C-0633

Task No. NR 051-690

TECHNICAL REPORT No. 7

Effects of Temperature on Excited-State Descriptions of Luminescent Photoelectrochemical Cells Employing Tellurium-Doped Cadmium Sulfide Electrodes

by

Arthur B. Ellis* and Bradley R. Karas

Prepared for Publication

in the

ACS Symposium Series, No. 146, "Photoeffects at Semiconductor-Electrolyte Interfaces", Arthur J. Nozik, Editor

Department of Chemistry
University of Wisconsin
Madison, Wisconsin 53706

October 6, 1981

Approved for Public Release: Distribution Unlimited

*To whom all correspondence should be addressed.

Unclassified

SECURITY CLASSIFICATION OF THIS PAGE (When Data Entered)

REPORT DOCUMENTATION PAGE		READ INSTRUCTIONS BEFORE COMPLETING FORM
1. REPORT NUMBER TECHNICAL REPORT NO. 7	2. GOVT ACCESSION NO. AD A107544	3. RECIPIENT'S CATALOG NUMBER
4. TITLE (and Subtitle) Effects of Temperature on Excited-State Descriptions of Luminescent Photoelectrochemical Cells Employing Tellurium-Doped Cadmium Sulfide Electrodes		5. TYPE OF REPORT & PERIOD COVERED 6. PERFORMING ORG. REPORT NUMBER
7. AUTHOR(s) Arthur B. Ellis and Bradley R. Karas		8. CONTRACT OR GRANT NUMBER(s) N00014-78-C-0633
9. PERFORMING ORGANIZATION NAME AND ADDRESS Department of Chemistry, University of Wisconsin, Madison, Wisconsin 53706		10. PROGRAM ELEMENT, PROJECT, TASK AREA & WORK UNIT NUMBERS NR 051-690
11. CONTROLLING OFFICE NAME AND ADDRESS Office of Naval Research/Chemistry Program Arlington, Virginia 22217		12. REPORT DATE October 6, 1981 13. NUMBER OF PAGES 13
14. MONITORING AGENCY NAME & ADDRESS(if different from Controlling Office)		15. SECURITY CLASS. (of this report) Unclassified 15a. DECLASSIFICATION/DOWNGRADING SCHEDULE

16. DISTRIBUTION STATEMENT (of this Report)

Approved for Public Release: Distribution Unlimited

17. DISTRIBUTION STATEMENT (of the abstract entered in Block 20, if different from Report)

18. SUPPLEMENTARY NOTES

Prepared for publication in the ACS Symposium Series, No. 146, "Photoeffects at Semiconductor-Electrolyte Interfaces", Arthur J. Nozik, Editor

19. KEY WORDS (Continue on reverse side if necessary and identify by block number)

Photoelectrochemistry; luminescence; doped cadmium sulfide electrodes

20. ABSTRACT (Continue on reverse side if necessary and identify by block number)

The effect of temperature on excited-state deactivation processes in a single-crystal, n-type, 100 ppm CdS:Te-based photoelectrochemical cell (PEC) employing aqueous polychalcogenide electrolytes is discussed. While serving as electrodes these materials emit (λ_{max} ~600 nm). Photocurrent (quantum yield ϕ) from ultraband gap (≥2.4 eV; $\lambda \leq$ 500 nm) 501.7 nm excitation increases modestly by ≤20% between 20° and 100°C; photocurrent from band

DD FORM 1 JAN 73 1473 EDITION OF 1 NOV 65 IS OBSOLETE
S/N 0102-LF-014-6601

Unclassified

SECURITY CLASSIFICATION OF THIS PAGE (When Data Entered)

gap edge 514.5 nm excitation increases by about an order of magnitude, reaching ~50-100% of the room temperature 501.7 nm value. Highlighting the competitive nature of emission and photocurrent as excited-state decay processes, luminescence (quantum yield ϕ_l) declines over the same temperature regime by factors of between 10 and 30. At most, modest red shifts of λ_{max} (<10 nm) are observed in the spectral distribution of emission with temperature. These effects are discussed in terms of optical penetration depth, band bending, and the known red shift of the CdS absorption edge with temperature. Correlations involving ϕ_x and ϕ_r suggested by the data are discussed.

The need for alternate energy sources has led to the rapid development of photoelectrochemical cells (PECs). A PEC consisting of an n-type semiconductor, a counterelectrode, and a suitably chosen electrolyte can convert optical energy directly into chemical fuels and/or electricity (1,2,3,4). We recently reported that tellurium-doped CdS (CdS:Te) mimics undoped CdS in its ability to sustain the conversion of monochromatic ultraband gap light ($\geq$2.4 eV; $\lambda \leq 500$ nm (5)) into electricity at $\sim$7% efficiency in PECs employing aqueous polychalcogenide electrolytes (6,7,8,9). A novel feature of the CdS:Te photoanodes is that they emit (λ_{max} $\sim$600 nm for 100 ppm CdS:Te) with $\sim$0.1% efficiency while effecting the oxidation of polychalcogenide species.

Luminescence results from the introduction of intraband gap states by the substitution of Te for S in the CdS lattice. Because of its lower electron affinity, Te sites trap holes which can then coulombically bind an electron in or near the conduction band to form an exciton. Subsequent radiative collapse of this exciton leads to emission (10,11,12,13). In the context of the PEC, emission thus serves as a probe of electron-hole ($e^- - h^+$) pair recombination which competes with $e^- - h^+$ pair separation leading to photocurrent. Except for intensity, the emitted spectral distribution is found to be independent of the presence and/or composition of polychalcogenide electrolyte, excitation wavelength (Ar ion laser lines, 457.9-514.5 nm) and intensity ($\leq$30 mW/cm^2), and applied potential (-0.3V vs. SCE to open circuit) (6,7,8,9).

Optical penetration depth plays a significant role in the PEC properties we observe. The absorptivity of 100 ppm CdS:Te for 514.5 nm light is $\sim 10^3$ cm^{-1} (5,10,11,12,13). Since the depletion region in which $e^- - h^+$ pairs are efficiently separated by band bending to yield photocurrent is $\sim 10^{-4}$-10^{-5} cm thick (14), a significant fraction of 514.5 nm light is absorbed beyond this region. We therefore expect and observe greater emission intensity and smaller photocurrent with 514.5 nm excitation than with ultraband gap wavelengths (8) for which the CdS:Te

absorptivity is $\sim 10^4$-10^5 cm^{-1} (5,10,11,12,13). Additionally, whereas there is little potential dependence of emission intensity with 514.5 nm excitation, a strong dependence is observed with ultraband gap irradiation: in passing from -0.3V vs. SCE to open circuit in aqueous polychalcogenide electrolytes, increases in emission intensity of ~15-1400% obtain (6,7,8,9). This is in accord with the premise that variations of potential correspond to alterations in the degree of band bending (14).

Temperature is another PEC parameter which can potentially modify the efficiencies of photocurrent and luminescence. Among the materials whose temperature dependent PEC properties have been studied are SnO_2 (15), TiO_2 (16) and $CuInS_2$ (17). Undoped CdS has a known optical band gap temperature dependence of -5.2×10^{-4} eV/°K between 90 and 400 K (18). Owing to the general similarity of CdS:Te to CdS, we anticipated a comparable red shift in the onset of absorption. In this paper we summarize the results of temperature studies on CdS:Te-based PECs employing aqueous polyselenide (9) and sulfide electrolytes.

Experimental

Single-crystal plates of vapor-grown, 100 ppm CdS:Te were purchased from Cleveland Crystals, Inc., Cleveland, Ohio. Emissive spectral features were consistent with those previously reported for CdS:Te (6-13) and confirmed (Roessler's correlation, (12)) that the Te concentration was ≤100 ppm. The ~5x5x1 mm samples had resistivities of ~2 ohm-cm (four point probe method) and were oriented with the 5x5 mm face perpendicular to the c-axis. Samples were first etched with 1:10 (v/v) Br_2/MeOH and then placed in an ultrasonic cleaner to remove residual Br_2. The electrolyte was either sulfide, 1M OH^-/1M S^{2-}, or polyselenide, typically 5M OH^-/0.1M Se^{2-}/0.001M Se_2^{2-}; short optical pathlengths (≤0.1 cm) were used to make the latter essentially transparent for $\lambda \geq 500$ nm. Electrode and electrolyte preparation as well as electrochemical and optical instrumentation employed have been described previously (8). Electrolytes were magnetically stirred and blanketed under N_2 during use.

Assembling the PEC inside the sample compartment of a spectrophotofluorometer permitted measurement of emission spectral data (200-800 nm; ~5 nm bandwidth). Front-surface emissive properties were recorded by inclining the photoelectrode at ~45° to both the incident Coherent Radiation CR-12 Ar ion laser beam (501.7 or 514.5 nm) and the emission detection optics. In all experiments the ~3 mm dia. beam was 10X expanded and masked to fill the electrode surface; incident intensities were generally ≤10 mW/cm^2. Temperature of the PEC was adjusted as previously described (9).

Results and Discussion

Emissive and Photocurrent Properties. Three characteristics of emissive PECs which might display thermal effects are the emissive spectral distribution, emission intensity, and photocurrent. We observed the emission spectrum of 100 ppm CdS:Te in both polyselenide and sulfide electrolytes from 20-100°C. Low-resolution spectra of the various samples revealed red-shifts of λ_{max} with increasing temperature of at most 5-10 nm; the displacement of λ_{max} for many samples, however, was within the bandwidth of the spectrometer (∿5 nm). These results are in the range of an extrapolation of Roessler's data (12) from which we would predict a red-shift in λ_{max} of ∿7-11 nm between 20 and 100°C. Parallel shifts have also been reported for CdS:Te absorption and excitation spectra over subambient temperature ranges (13). These spectra incorporate a low-energy band which distinguishes CdS:Te from CdS and, in fact, masks the exact position of the CdS:Te band gap (7,8,11,12,13). Several other features of the CdS:Te emission spectrum are particularly relevant in the context of PEC experiments. For a given temperature the spectral distribution is independent of whether 501.7 or 514.5 nm excitation is used and of electrode potential between +0.7 V vs. Ag (pseudoreference electrode, PRE) and the onset of cathodic current. Such an insensitivity to potential indicates that the energies of the intraband gap Te states are affected by potential in the same manner as the conduction and valence band energies.

A very profound temperature effect was observed for the emission intensity. Figure 1 presents an emission-temperature profile at open circuit in sulfide electrolyte; the relative invariance of the sample's spectral distribution with temperature allowed us to monitor emission intensity at the band maximum. Emission intensity was matched for 501.7 and 514.5 nm excitation at 20°C using ∿17 times as much 501.7 nm intensity. Over the 20-100°C excursion emission intensity is seen to drop by factors of ∿8 and 30 for 501.7 and 514.5 nm excitation, respectively. These factors are consistent with the 10- to 20-fold decline observed in polyselenide electrolyte; in those experiments there also appeared to be little potential dependence of the results (9). Similar thermal quenching data has been reported for dry CdS:Te samples irradiated with UV light (10,12,13), electron beams (11), and α particles (19). The temperature dependence of the decline in emission intensity has been linked to the ionization energy of the Te-bound hole, ∿0.2 eV (10,11,12,13,19).

Given the inherently competitive nature of emission and photocurrent, it should not be surprising that photocurrent was generally observed to increase with temperature. Figure 2 is a photocurrent-temperature profile obtained at +0.7 V vs. Ag (PRE) in sulfide electrolyte; the light intensity and sulfide concentration employed ensured that photocurrents were limited by excitation rate and not by mass transport, i.e., photocurrents

were not saturated with respect to light intensity and were not affected by stirring. At 20°C for matching intensities (ein/sec) ∿15 times the photocurrent is observed with ultraband gap 501.7 nm excitation as with band gap edge 514.5 nm light. As the temperature is increased to 100°C, a modest increase in 501.7 nm photocurrent is observed, while about an order of magnitude growth is obtained for 514.5 nm excitation. In fact, at 100°C the 514.5 nm photocurrent has reached ∿60% of the ultraband gap photocurrent. Similar effects were observed in polyselenide electrolyte for both CdS:Te and undoped CdS (9).

The photocurrent enhancement for 514.5 nm excitation is a predictable consequence of an absorption edge which red shifts with temperature: As the absorptivity for 514.5 nm light increases with temperature, progressively larger fractions of light will be absorbed in the depletion region. In this sense the accelerated decline in emission intensity observed for 514.5 nm relative to 501.7 nm excitation (Figure 1) may include a contribution reflecting decreasing optical penetration depth; weaker emission would be expected as 514.5 nm light acquires status as an ultraband gap wavelength, since near-surface nonradiative recombination sites could play a more significant role in excited-state deactivation (7,8). Although the rate at which 514.5 nm photocurrent increases with temperature is in reasonable accord with the CdS optical band gap temperature coefficient, the effect of potential-dependent absorptivity must be considered.

Electroabsorption measurements have been made on undoped CdS at room temperature. They reveal that for electric fields of $\sim 10^5$ V/cm, the change in absorptivity, $\Delta\alpha$, is $\sim +1 \times 10^3$ and -4×10^3 cm^{-1} at 515 and 500 nm, respectively (20). While this effect helps to blur the discrepancy in 514.5 and 501.7 nm optical penetration depths, the resultant absorptivities are still sufficiently disparate relative to the width of the depletion region to yield very different photocurrents at 295 K. To our knowledge electroabsorption data are not presently available for CdS:Te. A crude attempt to gauge the magnitude of this effect at 295 K for 514.5 nm light suggests it is small (8). In the absence of electroabsorption data over the 20-100°C range, however, the electric field and thermal effects are not completely decoupled and the results presented here should be so treated.

We should point out that the temperature effects on emission intensity and photocurrent are completely reversible. Although this result suggests that electrode stability obtains over the duration of the experiments, the properties measured may not be very sensitive to variations in surface or near-surface composition. There is now considerable evidence, in fact, that surface reorganization processes do occur in CdS- and CdSe- based PECs in polychalcogenide electrolytes (17, 21-26). In particular, the occurrence of such an exchange reaction for CdS:Te in polyselenide electrolyte would yield CdSe to whose lower band gap

(1.7 eV (27)) some of the observed properties could be attributed. The reversibility of the temperature effects as well as the similar behavior seen in sulfide electrolyte argue against such an explanation. Additionally, we have employed low light intensities ($\lesssim$10 mW/cm^2) and current densities ($\lesssim$2 mA/cm^2 with a total charge of generally $\lesssim$1 C/cm^2) to further minimize exchange processes. But we do recognize that our techniques by no means rule out the possibility of surface reorganization processes at some level.

Simultaneous measurement of current, luminescence and voltage can be presented in iLV curves which summarize much of our data. We find that the ratio of open-circuit to in-circuit luminescence intensity (ϕ_{r_o}/ϕ_r) is a useful expression of the emission's potential dependence, with the in-circuit value taken at a potential where the photocurrent is saturated. Low values of photocurrent quantum yield, $\phi_x \leq 0.1$, occur with band gap edge excitation and yield ϕ_{r_o}/ϕ_r values close to unity. Ultraband gap excitation generally yields $0.5 \leq \phi_x \leq 1.0$. Pulsing the electrode between open circuit and the potential corresponding to saturated photocurrent easily demonstrates the non-unity value of ϕ_{r_o}/ϕ_r. Since photocurrent quantum yield increases markedly with temperature for band gap edge illumination, we predict that ϕ_{r_o}/ϕ_r will exceed unity at elevated temperatures. Figure 3 presents full iLV curves for a CdS:Te-based PEC employing polyselenide electrolyte. Equivalent intensities (ein/sec) of 501.7 and 514.5 nm light were employed at both room and elevated temperatures (49°C for 501.7 nm; 86°C for 514.5 nm). These iLV curves may be summarized as follows: Photocurrent at 23°C is $\sim$18 times greater for 501.7 nm excitation (curve A vs. curve B) and open-circuit emission intensity is $\sim$5 times smaller (curve A' vs. curve B') than for 514.5 nm light. The ratio of ϕ_{r_o}/ϕ_r is 1.0 for 514.5 nm (curve B') and 3.5 (curve A') for 501.7 nm illumination. Increasing the temperature to 49°C increases the photocurrent from 501.7 nm light by $\sim$15% (curve C) and diminishes the luminescence intensity by a factor of 2. However, a similar ϕ_{r_o}/ϕ_r ratio of 3.4 obtains (curve C'). At 86°C the 514.5 nm photocurrent increases by a factor of almost 8 (curve D). Despite its approximately 10-fold drop in intensity, emission from 514.5 nm excitation now exhibits a potential dependence with a ϕ_{r_o}/ϕ_r value of 1.27 (curve D' - note 10X scale expansion). Similar non-unity ϕ_{r_o}/ϕ_r values were observed in sulfide electrolytes at temperatures exceeding $\sim$80°C.

Interrelationships of Excited-State Decay Routes. The iLV curves conveniently display the competitive nature of photocurrent and luminescence intensity as excited-state deactivation pathways. Our analysis is limited in the sense that we have obtained absolute numbers for ϕ_x but have had to content ourselves with relative ϕ_r measurements. We lack measures of nonradiative recombination efficiency (ϕ_{nr}), although they now appear to be

obtainable by the technique of photothermal spectroscopy (28,29). Treating these as the only possible decay routes yields eq. 1

$$\phi_x + \phi_r + \phi_{nr} = 1 \quad (1)$$

At open circuit $\phi_x = 0$ and photogenerated $e^- - h^+$ pairs are forced to recombine. The ratio of ϕ_r to ϕ_{nr} is shown to be wavelength dependent by comparing the open-circuit emission intensities of curve A' and curve B' in Figure 3. This ratio is also temperature dependent, as shown in Figure 1.

Correlation of ϕ_x, ϕ_r, and ϕ_{nr} involves knowing the relative extent to which nonradiatively and radiatively recombining $e^- h^+$ pairs are prevented from recombining, i.e., their relative contribution to photocurrent. Three possible schemes are: photocurrent, ϕ_x, interconverts (1) exclusively with ϕ_r; (2) exclusively with ϕ_{nr}; (3) with both ϕ_r and ϕ_{nr} such that $\phi_{nr} = k\phi_r$ for any ϕ_x.

Scheme 1 is unlikely because of the relative magnitudes of ϕ_r and ϕ_x. Measured values of ϕ_r and ϕ_x are 10^{-3} and 10^{-1}, respectively, for band gap edge excitation (8). In passing from +0.7 V vs. Ag (PRE) to open circuit, a ~100-fold increase in emission intensity is predicted. This is inconsistent with the insensitivity displayed in curve B', Figure 3. Scheme 2 argues that ϕ_r will be independent of potential. While it appears that curve B' (Figure 3) agrees with this, it is contradicted by curves A',C', and D'. Although not perfect, Scheme 3 is most compatible with our data. This assumption when combined with eq. 1 leads to a simple relationship for monochromatic excitation between ϕ_x and ϕ_{r_o}/ϕ_r:

$$\frac{\phi_{r_o}}{\phi_r} = \frac{1}{1-\phi_x} \quad (2)$$

Table I consists of a compilation of ϕ_{r_o}/ϕ_r ratios as a function of ϕ_x. Our results and those presented for p-GaP and n-ZnO are in rough agreement with this simple model (8,9,30,31,32). Construction of a more refined model awaits incorporation of other data (nonexponential lifetimes, electroabsorption, carrier properties, intensity effects, quantitative evaluation of ϕ_{nr} by photothermal spectroscopy, e.g.) and examination of other systems.

Acknowledgment

We are grateful to the Office of Naval Research for support of this work. BRK acknowledges the support of the Electrochemical Society through a Joseph W. Richard Summer Fellowship. David J. Morano, Daniel K. Bilich, and Holger H. Streckert are thanked for their assistance with some of the measurements.

Table I. Relationship Between ϕ_x and ϕ_{r_o}/ϕ_r[a]

ϕ_x	ϕ_{r_o}/ϕ_r
0.001	1.00
0.01	1.01
0.05	1.05
0.10	1.11
0.20	1.25
0.30	1.43
0.40	1.67
0.50	2.00
0.60	2.50
0.70	3.33
0.80	5.00
0.90	10.00
1.00	∞

[a]Calculated from eq.2 where ϕ_x is the photocurrent quantum yield, and ϕ_{r_o}/ϕ_r is the ratio of emission quantum yields between open circuit and the potential where ϕ_x is measured.

Abstract

The effect of temperature on excited-state deactivation processes in a single-crystal, n-type, 100 ppm CdS:Te-based photoelectrochemical cell (PEC) employing aqueous polychalcogenide electrolytes is discussed. While serving as electrodes these materials emit (λ_{max} ~600 nm). Photocurrent (quantum yield ϕ_x) from ultraband gap ($\geq$2.4 eV; $\lambda \leq$ 500 nm) 501.7 nm excitation increases modestly by $\leq$20% between 20° and 100°C; photocurrent from band gap edge 514.5 nm excitation increases by about an order of magnitude, reaching ~50-100% of the room temperature 501.7 nm value. Highlighting the competitive nature of emission and photocurrent as excited-state decay processes, luminescence (quantum yield ϕ_r) declines over the same temperature regime by factors of between 10 and 30. At most, modest red shifts of λ_{max} (<10 nm) are observed in the spectral distribution of emission with temperature. These effects are discussed in terms of optical penetration depth, band bending, and the known red shift of the CdS absorption edge with temperature. Correlations involving ϕ_x and ϕ_r suggested by the data are discussed.

Literature Cited

1. Bard, A.J. Science, 1980, 207, 139.
2. Memming, R. Electrochim. Acta, 1980, 25, 77.
3. Wrighton, M.S. Acc. Chem. Res., 1979, 12, 303.
4. Nozik, A.J. Ann. Rev. Phys. Chem., 1978, 29, 189.
5. Dutton, D. Phys. Rev., 1958, 112, 785.

6. Ellis, A.B.; Karas, B.R. J. Am. Chem. Soc., 1979, 101, 236.
7. Ellis, A.B.; Karas, B.R. Adv. Chem. Ser., 1980, 184, 185.
8. Karas, B.R.; Ellis, A.B. J. Am. Chem. Soc., 1980, 102, 968.
9. Karas, B.R.; Morano, D.J.; Bilich, D.K.; Ellis, A.B. J. Electrochem. Soc., 1980, 127, 1144.
10. Aten, A.C.; Haanstra, J.H.; deVries, H. Philips Res. Rep., 1965, 20, 395.
11. Cuthbert, J.D.; Thomas, D.G. J. Appl. Phys., 1968, 39, 1573.
12. Roessler, D.M. J. Appl. Phys. 1970, 41, 4589.
13. Moulton, P.F., Ph.D. Dissertation, Massachusetts Institute of Technology, 1975.
14. Gerischer, H. J. Electroanal. Chem., 1975, 58, 263.
15. Wrighton, M.S.; Morse, D.L.; Ellis, A.B.; Ginley, D.S.; Abrahamson, H.B. J. Am. Chem. Soc., 1976, 98, 44.
16. Butler, M.A.; Ginley, D.S. Nature, 1978, 273, 524.
17. Heller, A.; Miller, B. Adv. Chem. Ser., 1980, 184, 215.
18. Bube, R.H. Phys. Rev., 1955, 98, 431.
19. Bateman, J.E.; Ozsan, F.E.; Woods, J.; Cutter, J.R. J. Phys. D. Appl. Phys., 1974, 7, 1316.
20. Blossey, D.F.; Handler, P. in "Semiconductors and Semimetals"; Willardson, R.K., Beer, A.C.,Eds.; Academic Press, New York, 1972; Vol. 9, Chapter 3 and references therein.
21. Noufi, R.N.; Kohl, P.A.; Rodgers, J.W. Jr.; White, J.M.; Bard, A.J. J. Electrochem. Soc., 1979, 126, 949.
22. Heller, A.; Schwartz, G.P.; Vadimsky, R.G.; Menezes, S.; Miller, B. ibid., 1978, 125, 1156.
23. Cahen, D.; Hodes, G.; Manassen, J. ibid., 1978, 125, 1623.
24. Gerischer, H.; Gobrecht, J. Ber. Bunsenges Phys. Chem., 1978, 82, 520.
25. Hodes, G.; Manassen, J.; Cahen, D. Nature (London), 1976, 261, 403.
26. DeSilva, K.T.L.; Haneman, D. J. Electrochem. Soc., 1980, 127, 1554.
27. Wheeler, R.G.; Dimmock, J.O. Phys. Rev., 1962, 125, 1805.
28. Fujishima, A.; Brilmyer, G.H.; Bard, A.J. in "Semiconductor Liquid Junction Solar Cells", Heller, A., Ed.; Proc. Vol. 77-3: Electrochemical Society, Inc.: Princeton, N.J. 1977, p. 172.
29. Fujishima, A.; Maeda, Y.; Honda, K.; Brilmyer, G.H.; Bard, A.J. J. Electrochem. Soc., 1980, 127, 840.
30. Ellis, A.B.; Karas, B.R.; Streckert, H.H. Faraday Discuss. Chem. Soc., in press.
31. Beckmann, K.H.; Memming, R. J. Electrochem. Soc., 1969, 116, 368.
32. Petermann, G.; Tributsch, H.; Bogomolni, R. J. Chem. Phys., 1972, 57, 1026.

Figure Legends

Figure 1. Relative emission intensity monitored at 600 nm vs. temperature in 1M OH^-/1M S^{2-} electrolyte of CdS:Te excited at open circuit with 514.5 (squares) and 501.7 nm (circles) light in identical geometries. The excitation intensity at 501.7 nm is ∿17X that at 514.5 nm in order to approximately match room temperature emission intensities.

Figure 2. Relative photocurrent vs. temperature for the CdS:Te photoelectrode of Fig. 1 in 1M OH^-/1M S^{2-} electrolyte excited in identical geometries with equivalent intensities (ein/sec) of 514.5 nm (filled circles) and 501.7 nm (open circles) light at +0.7 V vs. Ag (PRE). The scale is such that the 25°C, 501.7 nm photocurrent has been arbitrarily set to 100 and corresponds to a current density of ∿0.38 mA/cm^2 and a photocurrent quantum yield of ∿0.66.

Figure 3. Current-luminescence-voltage (iLV) curves for a 100 ppm CdS:Te electrode in polyselenide electrolyte. Unprimed, solid-line curves are photocurrent (left-hand scale) and primed, dotted-line curves are emission intensity (right-hand scale) monitored at λ_{max} ∿600 nm. Curves A and A' result from excitation at 501.7 nm, 23°C; curves B and B' from 514.5 nm, 23°C; curves C and C', 49°C and 501.7 nm excitation; curves D and D', 86°C, 514.5 nm irradiation. Note that the ordinate of curve D' has been expanded by a factor of 10. Equivalent numbers of 501.7 and 514.5 nm photons were used to excite the photoelectrode in identical geometric configurations. The exposed electrode area is ∿0.41 cm^2, corresponding to an estimated ϕ_x for 501.7 nm excitation at 23°C and +0.7 V vs. Ag (PRE) of ∿0.50, uncorrected for solution absorbance and reflectance losses (9).

Fig. 1

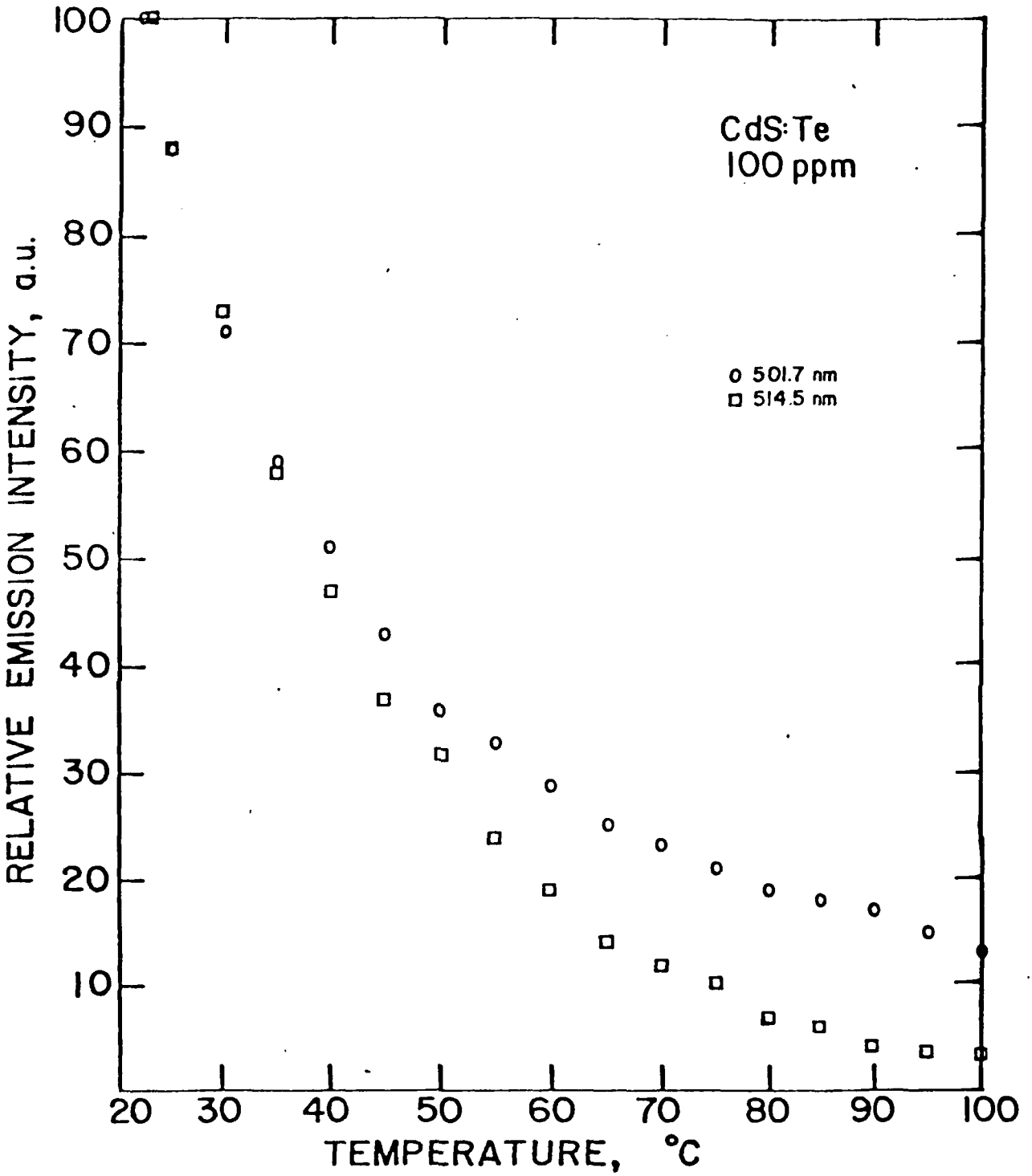
CdS:Te
100 ppm
o 501.7 nm
□ 514.5 nm
RELATIVE EMISSION INTENSITY, a.u.
TEMPERATURE, °C
100
90
80
70
60
50
40
30
20
10
20
30
40
50
60
70
80
90
100

Fig. 2

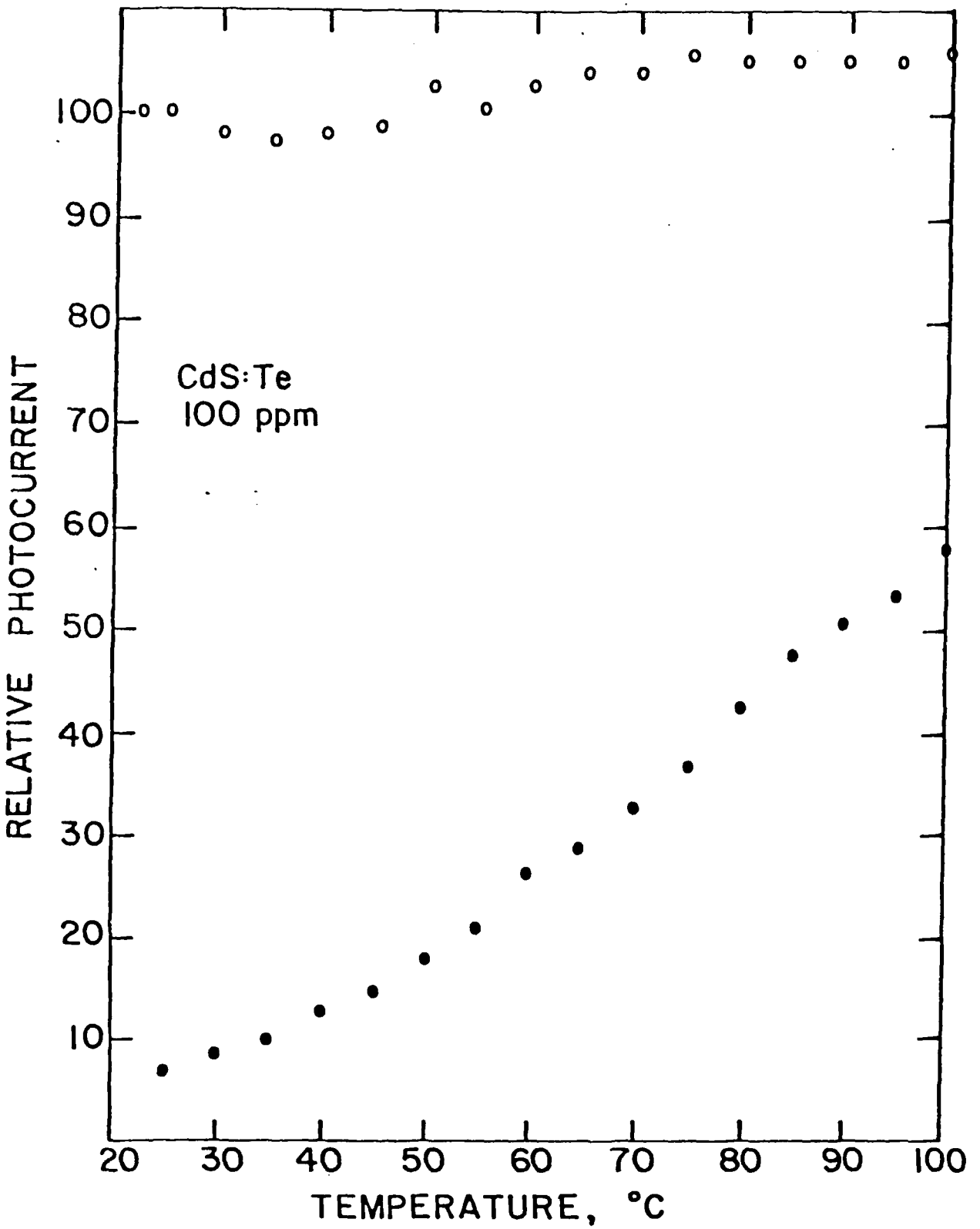
RELATIVE PHOTOCURRENT
100
90
80
70
60
50
40
30
20
10
CdS:Te
100 ppm
20
30
40
50
60
70
80
90
100
TEMPERATURE, °C

Fig. 3

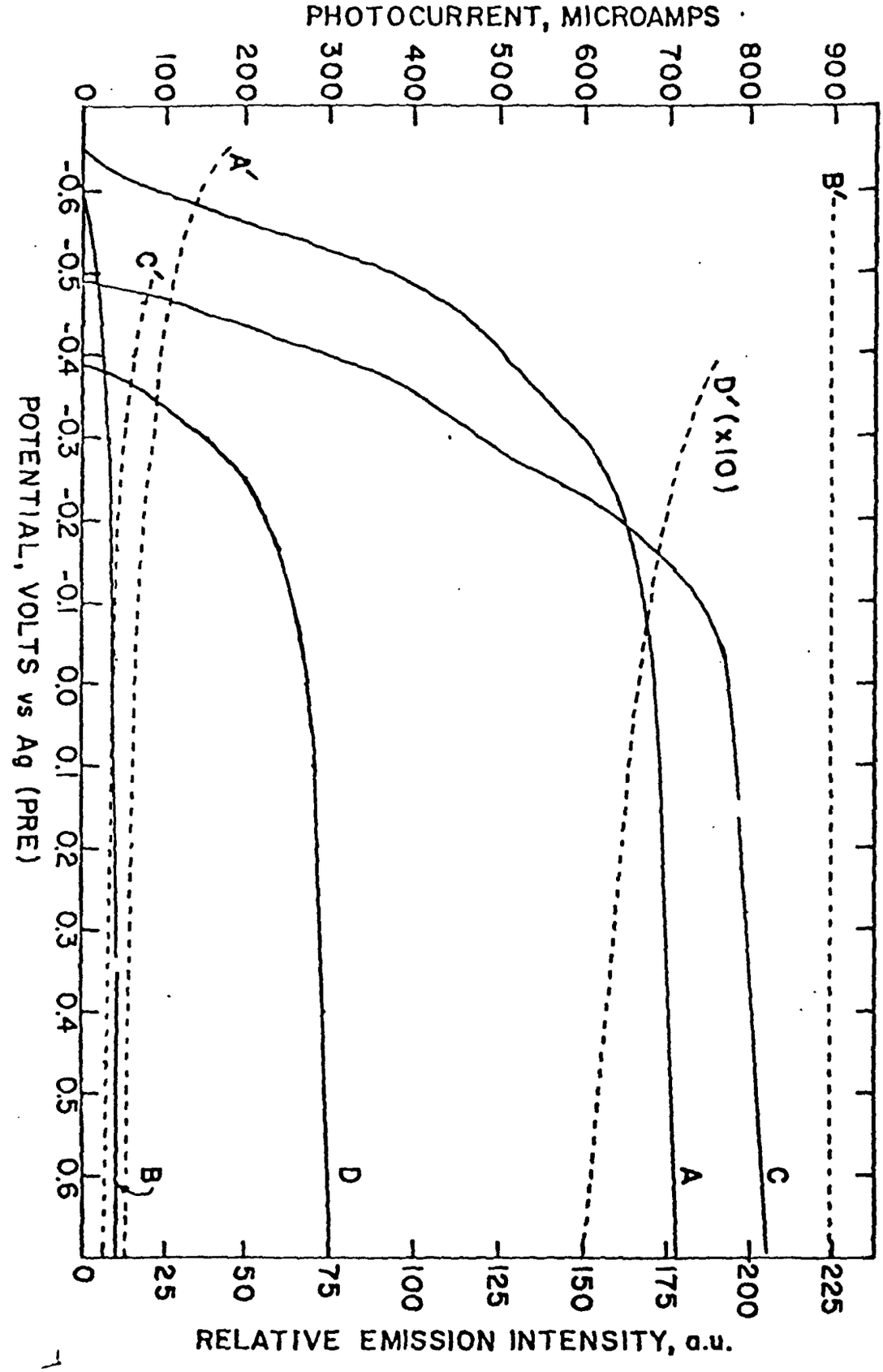
PHOTOCURRENT, MICROAMPS
0
100
200
300
400
500
600
700
800
900
POTENTIAL, VOLTS vs Ag (PRE)
-0.6
-0.5
-0.4
-0.3
-0.2
-0.1
0.0
0.1
0.2
0.3
0.4
0.5
0.6
A'
B'
C'
D'(x10)
A
B
C
D
0
25
50
75
100
125
150
175
200
225
RELATIVE EMISSION INTENSITY, a.u.


DA
FIL
2-